PCCP

PAPER

View Article Online
View Journal | View Issue

Cite this: *Phys. Chem. Chem. Phys.*, 2023, **25**, 6225

The stochastic wave function method for diffusion of alkali atoms on metallic surfaces

E. E. Torres-Miyares, *[a] D. J. Ward, [b] G. Rojas-Lorenzo, [c] J. Rubayo-Soneira, [cd] W. Allison[b] and S. Miret-Artés [ad]

Received 25th November 2022,
Accepted 28th January 2023

DOI: 10.1039/d2cp05511b

rsc.li/pccp

The stochastic wave function method is proposed to study the diffusion regimes of alkali atoms on metallic surfaces. The Lindblad approach, based on the microscopic Hamiltonian information in the Caldeira–Leggett model, is presented and numerical calculations of the dynamics are carried out to characterize surface diffusion for two different systems: Na–Cu(111) and Li–Cu(111). Calculations of the intermediate scattering function for an isolated adsorbate are compared, in the Brownian limit, with results deduced from helium spin-echo (HeSE) experiments after reducing them to single adsorbate dynamics. To illustrate the method we present the dependence on momentum transfer and the temperature dependency. Results show that the experiment can be described at a quantitative level by the 1-D quantum model (reduced dimensionality).

1 Introduction

The adsorption of alkali metal on metallic surfaces has technological impact on industrial catalytic processes.[1] For example, the presence of controlled quantities of alkali metals influences a variety of heterogeneous catalytic processes[2,3] and the complexity of the behaviour observed[4,5] is surprising given the relatively simple electronic structure in the alkali metal adsorption. Alkali metals tend to chemisorb at high symmetry sites without disturbing the underlying substrate[4] and, at low coverages, the valence charge of the alkali metal is shifted towards the substrate due to the difference in electron affinity leading to a dipole moment whereas, at high coverage, the alkali layer takes on a metallic character.[6,7] The adsorption site, itself, can depend on the coverage.[8]

Recent studies of the diffusion of alkali atoms on Cu(001) and Cu(111) surfaces include Na–Cu(111),[9] Na–Cu(001),[10–13] K–Cu(001)[14] and Li–Cu(001).[7] In addition to experiment, calculations[15,16] provide knowledge of both the adsorbate–substrate interaction and the inter-adsorbate forces giving information relevant to phenomena such as adsorption, desorption, dissociation and recombination.[17]

A description of the force fields (adsorbate–adsorbate and adsorbate–substrate interactions) is necessary to formulate the molecular dynamics of alkali metal on metallic surfaces. The Langevin formalism[18] provides a classical description that is sufficient in many situations.[19] Adsorbate–adsorbate interactions can be included explicitly[20] or treated approximately with an additional white shot noise.[21] Here, we treat the problem quantum-mechanically in one dimension (reduced dimensionality), using a new theoretical method that has been proposed by some of the present authors[22,23] in this context. We apply the method in the diffusive limit to discuss two systems for which new experimental data exist: Na–Cu(111) and Li–Cu(111). In the context of surface diffusion, the model has never been used and represents an alternative to the classical, Langevin formalism.

The work focuses on an interpretation of the dynamical behaviour in the limit of long-times, where the motion is primarily diffusive. In that limit, the dynamics are determined predominantly by the energy landscape and are insensitive to the spectrum of thermal excitations.[24] We extract the behaviour, at long-times, from the intermediate scattering function in both experiment and calculation before comparing the two. In addition, and where relevant, we eliminate the effect of adsorbate–adsorbate interactions from the experimental data through an effective incoherent intermediate scattering function in the neutron scattering context, using methods that have been described previously.[20]

Our primary aim, here, is to demonstrate that a fully quantum approach to diffusive dynamics is now a practical proposition for the analysis of experiment. Most previous work

[a] *Instituto de Física Fundamental, Consejo Superior de Investigaciones Científicas, Serrano 123, 28006, Madrid, Spain. E-mail: elena.torres@iff.csic.es, s.miret@iff.csic.es*
[b] *SMF Cavendish Laboratory, JJ Thomson Avenue, Cambridge, UK. E-mail: djw77@cam.ac.uk, wa14@cam.ac.uk*
[c] *Instituto Superior de Tecnologías y Ciencias Aplicadas (InSTEC),Universidad de La Habana, Avenida Allende No. 1110, Plaza, La Habana, 10400, Cuba. E-mail: grojas37@gmail.com, jrubayo@gmail.com*
[d] *Donostia International Physics Center (DIPC), Paseo Manuel de Lardizabal, 4, 20018, Donostia-San Sebastian, Spain*

has assumed classical behaviour, except in systems, such as the diffusion of atomic hydrogen at low temperatures, where quantum effects are expected to dominate. By demonstrating that the quantum calculations can represent experiments for light adsorbates, such as Li, as well as heavier adsorbates, such as Na, our work covers the regime where the validity of classical methods may be open to question.

The paper is organized as follows. In Section 2, the Caldeira–Leggett model, Lindblad theory and stochastic wave function method are presented as a theoretical model for the surface diffusion processes. In Section 3, new numerical and experimental results for two different systems, Na–Cu(111) and Li–Cu(111), are presented and compared with previous analytic results. Finally, in Section 4, the main conclusions of this work are summarized and future perspectives are presented.

2 The stochastic wave function method

The pioneering Caldeira–Leggett (CL) formalism is used to describe the motion of a quantum Brownian particle linearly coupled to an Ohmic environment in the weak-coupling and high-temperature limits.[25,26] Assuming short environmental correlation times and tracing out the environment degrees of freedom, a Markovian quantum master equation for the reduced density matrix is written for a one dimensional problem as[27]

$$\frac{\partial\rho(x,x',t)}{\partial t}=\left[-\frac{\hbar}{2mi}\left(\frac{\partial^2}{\partial x^2}-\frac{\partial^2}{\partial x'^2}\right)-\gamma(x-x')\left(\frac{\partial}{\partial x}-\frac{\partial}{\partial x'}\right)+\right.$$
$$\left.+\frac{V(x)-V(x')}{i\hbar}-\frac{D}{\hbar^2}(x-x')^2\right]\rho(x,x',t), \tag{1}$$

where V is the external interaction potential, is $\rho(x, x', t)$ represent the non-diagonal elements of the reduced density matrix, m is the particle mass, γ the friction coefficient and D the diffusion coefficient given by

$$D=2m\gamma k_{\mathrm{B}}T, \tag{2}$$

k_{B} being Boltzmanns constant and T the surface temperature.

However this formalism has a few drawbacks, the determinant of the generator of the CL master equation is negative and is only valid for high temperatures. Different attempts to obtain a master equation from microscopic Hamiltonians preserving the density positivity have been made.[28,29] Several works limited to the weak-coupling[30,31] or high-temperature regime[32] are found in the literature. A new approach using the quantum dynamical semigroups by Lindblad[29] and Kossakowski *et al.*[33] arrived to a generator of a completely positive map. Unlike closed systems where the dynamics can be described by the unitary time evolution, finding an appropriate equation of motion for the density matrix is the main goal. An open system can be represented as a system-plus-environment scheme. In this case, the dissipative evolution of the reduced density matrix depends on the Liouville functional $\mathfrak{L}$

$$\frac{\mathrm{d}\rho(t)}{\mathrm{d}t}+\frac{i}{\hbar}[\hat{H},\rho(t)]=\mathfrak{L}\rho(t), \tag{3}$$

where $\hat{H}$ is the Hamiltonian of the system. Lindblad and Kossakowski[29,33] presented a generator for a completely positive map in terms of operators $\hat{A}_k$

$$\mathfrak{L}\rho=\sum_k\left\{\left[\hat{A}_k,\rho\hat{A}_k^+\right]+\left[\hat{A}_k\rho,\hat{A}_k^+\right]\right\}, \tag{4}$$

known as Lindblad dissipation operators. Replacing (4) in (3), the Lindblad equation is then written as

$$\frac{\mathrm{d}\rho(t)}{\mathrm{d}t}+\frac{i}{\hbar}[\hat{H},\rho(t)]=\sum_k\left\{\left[\hat{A}_k,\rho\hat{A}_k^+\right]+\left[\hat{A}_k\rho,\hat{A}_k^+\right]\right\}. \tag{5}$$

The structure of the operators $\hat{A}_k$ is unknown but it can be found based on the microscopic Hamiltonian information coming from the CL formalism.

The minimal invasive modification to the CL master eqn (1) can be carried out by just adding an additional term of the form $\gamma[\hat{p},[\hat{p},\rho]]/8mk_{\mathrm{B}}T$, which is small in the high temperature limit,

$$\frac{\mathrm{d}\rho}{\mathrm{d}t}=-\frac{i}{\hbar}[\hat{H},\rho]-\frac{i\gamma}{2\hbar}[\hat{x},\{\hat{p},\rho\}]-\frac{2m\gamma k_{\mathrm{B}}T}{\hbar^2}[\hat{x},[\hat{x},\rho]]+$$
$$+\frac{\gamma}{8mk_{\mathrm{B}}T}[\hat{p},[\hat{p},\rho]]. \tag{6}$$

From eqn (6), the CL master equation can be brought into Lindblad form (5) for one Lindblad operator $\hat{A}_k$ given by a linear combination of the position $\hat{x}$ and momentum $\hat{p}$ operators,

$$\hat{A}=\mu\hat{x}+i\nu\hat{p},\ \hat{A}^+=\mu\hat{x}-i\nu\hat{p} \tag{7}$$

Replacing the operators (7) in the Lindblad eqn (5), the corresponding Markovian master equation is

$$\frac{\mathrm{d}\rho}{\mathrm{d}t}+\frac{i}{\hbar}[\hat{H}',\rho]=-\mu^2[\hat{x},[\hat{x},\rho]]-2i\mu\nu\left[\hat{x},[\hat{p},\rho]_+\right]-\nu^2[\hat{p},[\hat{p},\rho]],$$
$$\hat{H}'=\hat{H}-2\mu\nu\hbar\hat{x}\hat{p}. \tag{8}$$

In the coordinate space, this equation takes the following expression

$$\frac{\partial\rho}{\partial t}(x,x',t)+\frac{i}{\hbar}[\tilde{H}(x)-\tilde{H}^*(x')]\rho(x,x',t)=-\{\mu^2(x-x')^2+$$
$$+\gamma(x-x')\left(\frac{\partial}{\partial x}-\frac{\partial}{\partial x'}\right)-\nu^2\hbar^2\left(\frac{\partial}{\partial x}+\frac{\partial}{\partial x'}\right)^2\}\rho(x,x',t). \tag{9}$$

A simplest way to solve the master eqn (9) is using a set of stochastic wave functions $\{|\psi\rangle\}$, where each function obeys the following differential equation

$$d|\psi\rangle=-\frac{i}{\hbar}\hat{H}|\psi\rangle\mathrm{d}t-\left[\mu^2(\hat{x}-\bar{x})^2+\nu^2(\hat{p}-\bar{p})^2+\frac{i\gamma}{\hbar}(\bar{p}\hat{x}-\bar{x}\hat{p})\right]\times$$
$$\times|\psi\rangle\mathrm{d}t+[\mu(\hat{x}-\bar{x})+i\nu(\hat{p}-\bar{p})]|\psi\rangle\mathrm{d}\xi, \tag{10}$$

where $\bar{x} = \langle\psi|\hat{x}|\psi\rangle$, $\bar{p} = \langle\psi|\hat{p}|\psi\rangle$ and $d\xi$ are complex stochastic variables fulfilling the properties of a Wiener process $d\xi$ (the mean and variance of fluctuations are zero and $dt^{1/2}$, respectively): $M\left[d\xi_k d\xi_n^*\right] = 2dt\delta_{kn}$, $M\left[d\xi_k^* d\xi_n^*\right] = 0$ and $M[d\xi_k d\xi_n] = 0$, where M stands for a mean over fluctuations due to the stochastic process.[34] Eqn (10) is known as the Îto stochastic differential equation.

Previously, the Îto stochastic differential equation has only been applied to a limited number of adsorbate systems. The idealised vibrational relaxation and desorption of O_2–Pt(111) have been discussed by Gao,[28] while some of the present authors have studied Xe–Pt(111).[22,23] Here, we apply a similar method to the dynamics of sodium and lithium atoms, in the diffusive regime on a copper surface in order to compare them directly with information extracted from new and recent helium spin-echo experiments.

3 Experiment and numerical results

3.1 Experiment

Experimental data for both Na/Cu(111) and Li/Cu(111) are obtained from helium spin-echo (HeSE) measurements using an incident energy $E_i \simeq 8$ meV, and at a surface coverage of $\theta \simeq 0.025$ ML. Surface temperatures for the data presented here were $T_s = 155$ K for the Na case and $T_s = 140$ K for the Li case. Measurements for Na/Cu(111) have been described previously.[9,20] The Li/Cu(111) data are obtained and analysed in a similar manner. Specifically, the experiment generates a normalised intermediate scattering function (ISF) corresponding to coherent scattering from all features on the surface. Static features, such as surface steps or point defects, give a constant, time-independent contribution to the ISF which is removed by fitting a constant background. Features due to inelastic scattering, such as those generated by single-phonon scattering add a periodic contribution that can be removed effectively by Fourier filtering in the energy-domain.[9] The remaining features are attributed to quasi-elastic scattering from the ballistic and diffusive motion of the adsorbates. The mean rate of energy transfer, γ, between an adsorbate and the heat-bath of the substrate acts to distinguish between ballistic motion, which dominates at short times, $t \ll 1/\gamma$, and diffusive motion, which is predominant at long times, $t \gg 1/\gamma$. In the present work, we are concerned with diffusive motion and thus extract the necessary information from the long-time behaviour of the ISFs. The procedure used to analyse diffusive motion is described in detail in Rittmeyer *et al.*,[9] and, for Na/Cu(111), we obtain the characteristic decay rates of the diffusive correlations by excluding data for $t < 18$ ps. In all of the data below, we assume an exponential time dependence of the form $I(\Delta\mathbf{K}, t) \sim \exp(-\alpha(\Delta\mathbf{K})t)$, where the dephasing rate, α, is presented as a function of $\Delta\mathbf{K}$.

In the case of Na/Cu(111), one further step of analysis is necessary before the experiment can be compared with the calculations. The numerical method describes correlations in the motion of a single diffusing entity whereas the experiment necessarily involves many adsorbates. Spatial correlations observed in the experiment include a self-part, which tracks the correlation of an individual particle, and a distinct-part, which tracks the pairwise correlations with other particles.[35] For Na/Cu(111), the inter-adsorbate forces are significant and we extract the self-correlations assuming pairwise forces and a power-law form-factor,[20] before comparison with the calculations.

3.2 Numerical results

In order to solve the Îto stochastic differential eqn (10) we have used the split operator method described in ref. 36. As seen in previous works,[37] the Lindblad operators coefficients have been taken as $\mu = \sqrt{4mk_BT/\hbar^2}$ and $\nu = \sqrt{1/4mk_BT}$. In this way, the temperature has been incorporated in the system description. Position $\hat{x}$ and momentum $\hat{p}$ operators are propagated in the coordinate and momentum space, respectively. The numerical code was developed to solve, N times, the stochastic differential eqn (10). In order to obtain the observables average values, the number of realizations N is chosen to be large enough to reach the numerical stability and convergence.

The discrete wave function $\psi(x, t)$ is evaluated, at each time t, in equally spaced points belonging to the interval $[x_1, x_{N_s}]$, N_s being the number of points a power of 2 (in this way the fast Fourier transform can be used when necessary)

$$\psi(x, t) \equiv \{\psi(x_1, t); \psi(x_2, t); \psi(x_3, t); \cdots; \psi(x_{N_s}, t)\} \quad (11)$$

The wave function normalization is calculated as

$$F_{\text{norm}} = \sqrt{\sum_{i=1}^{N_s} \psi^*(x_i, t)\psi(x_i, t)\Delta x}, \quad (12)$$

where Δx is the length between two consecutive points of the grid. Each normalized stochastic wave function ($n = 1, \cdots N$) is then written as

$$\psi_n(x_i, t) = \frac{\psi(x, t)}{F_{\text{norm}}}, \quad (13)$$

and the mean value of any operator $\hat{B}$ for the N realizations can be expressed as

$$\left\langle \hat{B}(t) \right\rangle = \frac{1}{N} \sum_{n=1}^{N} \sum_{i=1}^{N_s} \psi_n^*(x_i, t) \hat{B}(t) \psi_n(x_i, t) \Delta x. \quad (14)$$

The ISF is a key quantity in the surface diffusion context and, for a single adsorbate, the ISF can be written as.

$$I(\Delta\mathbf{K}, t) = \left\langle e^{-i\Delta\mathbf{K}\cdot\hat{\mathbf{R}}(0)} e^{i\Delta\mathbf{K}\cdot\hat{\mathbf{R}}(t)} \right\rangle \quad (15)$$

For our problem, $\Delta\mathbf{K} = \Delta K$ is the wave vector transfer parallel to the surface, $\hat{\mathbf{R}}(t) = \hat{x}(t)$ and $\hat{\mathbf{R}}(0) = \hat{x}(0)$ are the position operators of the adatom/adsorbate at time t and $t = 0$, respectively. The x-dimension is considered as one of the symmetry

directions of the surface, where the projection on the wave vector transfer is carried out. Now, from eqn (15) we have that

$$I(\Delta K, t) = \frac{1}{N}\sum_{n=1}^{N}\langle\psi_n(x,t)|\mathrm{e}^{-i\Delta K[\hat{x}(t)-\hat{x}(0)]}|\psi_n(x,t)\rangle, \qquad (16)$$

where the mean value of the operator $\mathrm{e}^{-i\Delta K[\hat{x}(t)-\hat{x}(0)]}$ and $\hat{x}$ can be obtained from eqn (14). Thus, the ISF $I(\Delta K, t)$ is then calculated according to

$$I(\Delta K, t) = \frac{1}{N}\sum_{n=1}^{N}\left(\sum_{i=1}^{N_s}\left(\psi_n^*(x_i,t)\mathrm{e}^{-i\Delta K[x_i(t)-x(0)]}\psi_n(x_i,t)\Delta x\right)\right) = \frac{1}{N}\sum_{n=1}^{N} I_n(\Delta K, t), \qquad (17)$$

where $I_n(\Delta K, t)$ is the ISF of each stochastic realization. These values are calculated independently and summed up to give the average value, or $I(\Delta K, t)$.

The unidimensional space is chosen to be $x \in [-80, 80]$ Å, with a number of points $N_s = 4096$ and a number of realizations $N = 20\,000$. The increment Δx, given by $\Delta x = (x_f - x_i)/N_s$, for these parameters, is $\Delta x = 0.04$ Å. The initial wave function is considered to be a Gaussian wafunction given by

$$\psi(x,0) = \sqrt[4]{\frac{1}{2\pi\sigma_0^2}}\exp\left[-\frac{(x-x_0)^2}{2\sigma_0} + \frac{i}{\hbar}p_0(x-x_0)\right], \qquad (18)$$

where the initial position is chosen to be $x_0 = 0$ and the width $\sigma_0 = 0.1$ a.u. The velocities are distributed according to the Maxwell–Boltzmann distribution with mean $\sqrt{2k_BT/m}$ at a temperature T and the adsorbate with mass m. The time integration step chosen is $\Delta t = 66.1462$ a.u. = 1.6 fs in order to reach numerical convergence for the ISF.

3.3 Diffusion of Na on Cu(111)

In the stochastic wave function calculations, a potential with a single Fourier component and the periodicity of the substrate is assumed

$$V(x) = -\frac{E_b}{2}\cos\left(\frac{4\pi}{\sqrt{3}a}x\right), \qquad (19)$$

where $a = 3.615$ Å is the lattice constant. Simulation parameters are selected to match the conditions in the experiment.[9,38] The temperature was set at $T = 155$ K and the friction coefficient $\gamma = 0.20$ ps^{-1}. The energy barrier for this potential $E_b = 55$ meV coincides with the Langevin molecular simulations.[38]

At long times $t \gg \gamma^{-1}$ (say ten times γ^{-1}), the ISF is expected to decay as an exponential function $I(t) \sim \exp(-\alpha t)$, where the dependence of α on the scattering momentum-transfer, ΔK, provides information about the rate and nature of the diffusive motion. Fig. 1 shows decay rates $\alpha(\Delta K)$ from the stochastic wave function formalism (grey points) in comparison with experimental results (red points). The blue curve in Fig. 1

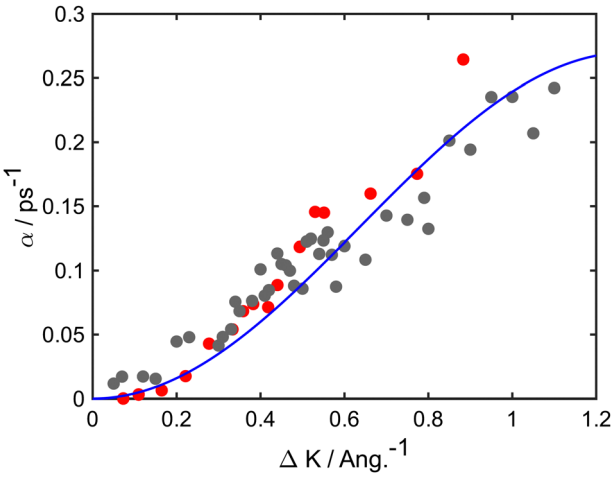

Fig. 1 Decay rate α of the Brownian component in the ISF, as a function of momentum transfer ΔK for Na adsorbates on Cu(111) surface at $T_s = 155$ K. Numerical calculations (grey points) are shown for simulations up to 50 ps using a friction $\gamma = 0.20$ ps^{-1} and an energy barrier $E_b = 55$ meV. Experimental data (red points) are for dephasing rates of single adsorbate dynamics.[20] The solid blue curve corresponds to idealised single-jumps (see text) and illustrates that the long-time dynamics of the system is described well by the classical Chudley–Elliott model.

corresponds to the analytic result for single hops obtained using the Chudley–Elliott model,[39] which has the form

$$\alpha(\Delta K) = \frac{2}{\tau}\sin^2\frac{\Delta K}{2}, \qquad (20)$$

where $1/\tau$ is the jump rate. The numerical results agree with the experimental data demonstrating that the quantum treatment represents the experiment well. In addition, both data sets are represented well by the Chudley–Elliott blue curve for single-hops between nearest-neighbour sites. Such an agreement is significant since it illustrates the calculations are in a regime whose classical description could be characterised as being dominated by single, over-barrier hops between nearest-neighbour sites.

Stochastic wave function calculations also reproduce the temperature dependence observed in experiment, which over a limited temperature range is well represented by an Arrhenius law

$$\alpha(T) = \alpha_0\exp\left(-\frac{E_a}{k_BT}\right), \qquad (21)$$

where α is the decay rate and E_a is the effective activation energy. Fig. 2 shows an Arrhenius plot, which compares the numerical calculations (grey points) with experimental results (red points). The solid blue line is a regression line with a gradient corresponding to 14 meV. It is clear that the correct temperature dependence is well represented by the numerical simulations.

3.4 Diffusion of Li on Cu(111)

Simulations and experiment for the case of Li diffusion are analysed in a similar manner to those for Na. In the case of the experiment, there is little evidence for collective motion and so we compare the experimental $\alpha(\Delta K)$ directly with values derived

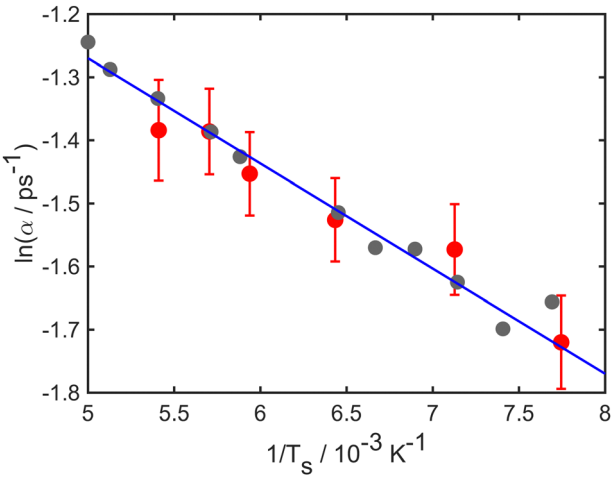

Fig. 2 Natural log of the decay rate log(α), as a function of the inverse temperature $1/T$ for the Na–Cu(111) system with a momentum transfer ΔK = 1.25 Å^{-1} for a corrugated surface with an energy barrier E_b = 55 meV and a friction coefficient γ = 0.20 ps^{-1}. Numerical results (grey points), experimental results (red points) and a linear regression line (solid blue line).

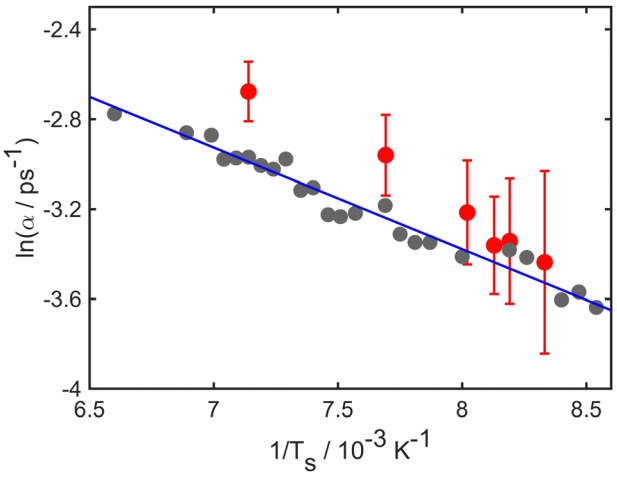

Fig. 4 Natural log of the decay rate ln(α), as a function of the inverse temperature $1/T$ for the Li–Cu(111) system with a momentum transfer ΔK = 1.0 Å^{-1}. Numerical results are shown as (grey points), experimental results shown as red points and the solid blue curve shows a linear dependence corresponding to an effective barrier of 41 meV.

from the numerical simulations. Both experiment and simulations correspond to T = 140 K, and, in the simulations, the energy barrier is E_b = 45 meV, the friction coefficient is γ = 1.20 ps^{-1} and the values of α extracted from data up to 20 ps.

Fig. 3 shows a comparison of the simulations and experiment, which are shown, respectively, as grey and red data-points. The solid blue line is a guide to the eye and is included to facilitate comparison of the two data-sets. Simulations follow the experimental trend closely, and show somewhat less scatter than the experiment. Notice that the trends in both simulation and experiment, as represented by the solid line, are quite different to those in the case of Na/Cu(111), above. We conclude that the motion of the lithium atoms is not in the same "classical" regime of single-hops that was evident for Na and, therefore, some aspects of the dynamics are in a "quantum" regime. The close agreement of simulation and experiment, seen in Fig. 3 as well as Fig. 1, demonstrates the ability of the simulations to reproduce trends in both quantum and classical regimes.

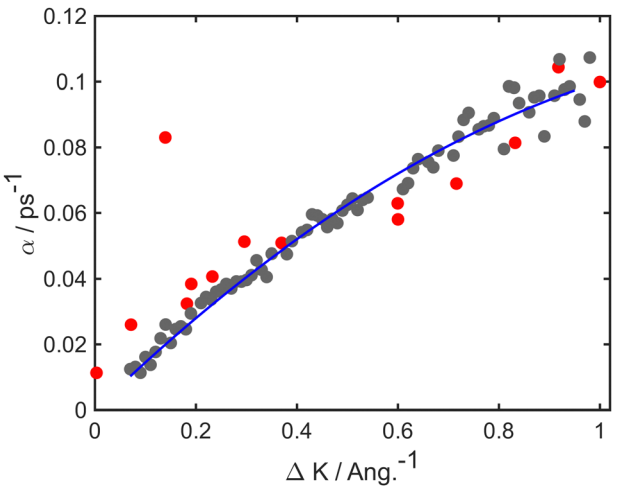

Fig. 3 Decay rate, α, as a function of momentum transfer, ΔK, for Li adsorbates on Cu(111); numerical results (grey points), experimental results (red points). The solid blue curve is included as a guide for the eye to facilitate comparison of simulation and experiment. The overall trend of the line does not follow a conventional dynamical signature such as that illustrated by the example of Na/Cu(111) in Fig. 1. In the simulations an energy barrier of E_b = 45 meV with friction γ = 1.20 ps^{-1} was used. Numerical results up to 20 ps are considered to extract the Brownian component of the motion.

The temperature dependence of the diffusive motion is illustrated in Fig. 4, which shows an Arrhenius plot for the temperature dependence of the decay rate. Log(α), is plotted against the inverse temperature $1/T$. Numerical results (grey points) and experimental results (red points) both have linear trends as expected from the Arrhenius law. The solid blue line shows a fit to the simulations data and corresponds to an effective activation energy of 41 meV. Notice, however, that the trend in the experiment suggests a somewhat steeper slope than that used to reproduce the simulations.

4 Conclusions

The stochastic wave function method has been used to analyze the surface diffusion of alkali atoms on a metallic surface. Both Na/Cu(111) and Li/Cu(111) have been studied and the results of simulations compared directly with experiment. In particular, we have obtained the time dependency of the intermediate scattering function in the Brownian regime, *i.e.* for times $t \gg 1/\gamma$, where γ is the mean rate of energy transfer. In both systems, agreement is evident in the ΔK dependence of the correlation decay-rate, α, as well as its temperature dependence. Na/Cu(111) is confirmed as a high friction system where the $\alpha(\Delta K)$ dependence follows the expectation for a classical atom performing single-hops between nearest-neighbour sites. In the case of

Li/Cu(111), the $\alpha(\Delta K)$ dependence does not follow any simple analytic model (for example, the Chudley–Elliott model), indicating that the diffusion cannot be explained simply in terms of the behaviour of a classical particle. The precise effects responsible for such an $\alpha(\Delta K)$ dependence are not obvious; however, they are reproduced well by the quantum calculations. Thus, we have demonstrated the stochastic wave function method can represent a "classical" regime as well as the quantum one, though clearly our future understanding could be improved given a larger experimental and computational data-set.

In our calculations we use a 1D potential, to represent the dynamics. The adsorbate, however, moves in 2D so the question of higher dimensionality is significant. Clearly, quantum motion along a reaction coordinate will be affected by the form of the potential in an orthogonal direction and the effect may be significant. A prominent example is that of inverse isotope effects in H/D motion,[40,41] where a constricted transition state can increase the local zero-point energy to the extent that lighter adsorbates have a lower transition rate than a heavier isotope. Even in such extreme cases it is still viable to describe the motion within a 1D potential, but with an effective barrier that is mass dependent. For this reason, the calculated potentials we use to describe the data should be regarded as effective potentials rather than the true adiabatic potential energy.

Furthermore, the success of our numerical approach suggests its extension further into the 2D quantum regime, where very light adsorbates, such as atomic hydrogen, are known to tunnel through the diffusion barrier. Work in this direction is now in progress.

Author contributions

All authors have contributed equally to this work.

Conflicts of interest

There are no conflicts to declare.

Acknowledgements

E. E. T.-M. and S. M. A. would like to thank Fundación Humanismo y Ciencia for financial support. G. R.-L. and J. R.-S. would also thank the Advanced Computational Team at Higher Institute for Technologies and Applied Sciences (Havana University) for the support provided during the realization of this work and to Project NA223LH-INSTEC-003. The authors acknowledge use of and support by the Cambridge Atom Scattering Facility (**https://atomscattering.phy.cam.ac.uk**) and EPSRC award EP/T00634X/1.

References

1 W. D. Mross, Alkali doping in heterogeneous catalysis, *Catal. Rev.: Sci. Eng.*, 1983, **25**(4), 591–637.
2 I. Waluyo, K. Mudiyanselage, F. Xu, W. An, P. Liu, J. A. Boscoboinik, J. A. Rodriguez and D. J. Stacchiola, Potassium-promoted reduction of Cu2O/Cu (111) by CO, *J. Phys. Chem. C*, 2019, **123**, 8057–8066.
3 R. Qin, L. Zhou, P. Liu, Y. Gong, K. Liu, C. Xu, Y. Zhao, L. Gu, G. Fu and N. Zheng, Alkali ions secure hydrides for catalytic hydrogenation, *Nat. Catal.*, 2020, **3**, 703–709.
4 R. D. Diehl and R. McGrath, Structural studies of alkali metal adsorption and coadsorption on metal surfaces, *Surf. Sci. Rep.*, 1996, **23**, 43–171.
5 R. D. Diehl and R. McGrath, Current progress in understanding alkali metal adsorption on metal surfaces, *J. Phys.: Condens. Matter*, 1997, **9**, 951–968.
6 P. Fouquet and G. Witte, Observation of metallization transition of 2D alkali metal films, *Phys. Rev. Lett.*, 1999, **83**, 360–363.
7 D. A. MacLaren, W. Luo, G. P. Brivio, C. Huang, G. Fratesi and W. Allison, Charge redistribution in the formation of one-dimensional lithium wires on Cu(001), *Phys. Rev. B: Condens. Matter Mater. Phys.*, 2010, **82**(8), 081413.
8 A. Spreinat, D. J. Ward, W. Allison, J. Ellis, A. P. Jardine, M. Sacchi, A. Raghavan, L. Slocombe and N. Avidor, Alkali metal adsorption on metal surfaces: new insights from new tools, *Phys. Chem. Chem. Phys.*, 2021, **23**, 7822–7829.
9 S. P. Rittmeyer, D. J. Ward, P. Gütlein, J. Ellis, W. Allison and K. Reuter, Energy dissipation during diffusion at metal surfaces: Disentangling the role of phonons versus electron-hole pairs, *Phys. Rev. Lett.*, 2016, **117**, 196001.
10 J. P. Toennies, L. Y. Chen, A. P. Graham, F. Hofmann and S. C. Ying, Determination of the Na/Cu(001) potential energy surface from helium scattering studies of the surface dynamics, *Phys. Rev. Lett.*, 1997, **78**(20), 3900.
11 H. Hedgeland, W. Allison, G. Alexandrowicz, A. P. Jardine and J. Ellis, Onset of 3D collective surface diffusion in the presence of lateral interactions: Na/Cu(001), *Phys. Rev. Lett.*, 2006, **97**(15), 156103.
12 A. S. Sanz, R. Martínez-Casado, J. L. Vega and S. Miret-Artés, Line shape broadening in surface diffusion of interacting adsorbates with quasielastic He atom scattering, *Phys. Rev. Lett.*, 2007, **98**(21), 216102.
13 M. I. Trioni, G. P. Brivio, G. Fratesi, G. Alexandrowicz and W. Allison, Crucial electronic contributions to measures of surface diffusion by he atom scattering, *Phys. Rev. B: Condens. Matter Mater. Phys.*, 2008, **77**, 235444.
14 H. R. Davies, A. P. Jardine, G. Alexandrowicz, W. Allison, J. Ellis, G. Fratesi, H. Hedgeland, P. R. Kole and G. P. Brivio, Surface dynamics and friction of K/Cu(001) characterized by helium-3 spin-echo and density functional theory, *Phys. Rev. B: Condens. Matter Mater. Phys.*, 2009, **80**(12), 125426.
15 A. Toro-Labbé and L. Padilla-Campos, Theoretical study of the diffusion of alkali metals on a Cu(111) surface, *J. Mol. Struct.: THEOCHEM*, 1997, **390**(1–3), 183–192.
16 G. Fratesi, Potential energy surface of alkali atoms adsorbed on Cu(001), *Phys. Rev. B: Condens. Matter Mater. Phys.*, 2009, **80**(045422), 8.
17 N. H. March, V. Bortolani and M. P. Tosi, *Interaction of atoms and molecules with solid surfaces*, Springer Science & Business Media, 2013.
18 J. Ellis and A. P. Graham, The use of quasielastic helium atom scattering to study correlated motion in adsorbate overlayers, *Surf. Sci.*, 1997, **377–379**, 833–842.

19 R. Ferrando, M. Diamant, S. Rahav and G. Alexandrowicz, Interpretation of surface diffusion data with Langevin simulations: a quantitative assessment, *J. Phys.: Condens. Matter*, 2015, **27**, 125008.
20 A. Tamtögl, A. P. Jardine, E. Bahn, J. Ellis, S. Miret-Artés, D. J. Ward, A. Raghavan and W. Allison, Inter-adsorbate forces and coherent scattering in helium spin-echo experiments, *Phys. Chem. Chem. Phys.*, 2021, **23**, 7799.
21 A. S. Sanz, R. Martínez-Casado, J. L. Vega and S. Miret-Artés, Surface diffusion and low vibrational motion with interacting adsorbates: A shot noise description, *Phys. Rev. E: Stat., Nonlinear, Soft Matter Phys.*, 2007, **75**, 051128.
22 E. E. Torres-Miyares, G. Rojas-Lorenzo, J. Rubayo-Soneira and S. Miret-Artés, Surface diffusion by means of stochastic wave functions. the ballistic regime, *Mathematics*, 2021, **9**(4), 362.
23 E. E. Torres-Miyares, G. Rojas-Lorenzo, J. Rubayo-Soneira and S. Miret-Artés, Surface diffusion within the Caldeira-Leggett formalism, *Phys. Chem. Chem. Phys.*, 2022, **24**(26), 15871–15890.
24 P. Hänggi and P. Jung, Colored noise in dynamical systems, *Adv. Chem. Phys.*, 2007, **89**, 239–326.
25 R. Feynman and R. B. Leighton, *The Brownian movement, Feynman lectures of physics*, 1964, vol. 1, p. 41.
26 U. Weiss, *Quantum Dissipative Systems*, World Scientific Publishing, Singapore, 2nd edn, 1999.
27 A. O. Caldeira and A. J. Leggett, Quantum tunnelling in a dissipative system, *Ann. Phys.*, 1983, **149**(2), 374–456.
28 S. Gao, Lindblad approach to quantum dynamics of open systems, *Phys. Rev. B: Condens. Matter Mater. Phys.*, 1998, **57**(8), 4509.
29 G. Lindblad, On the generators of quantum dynamical semigroups, *Commun. Math. Phys.*, 1976, **48**(2), 119–130.
30 S. Gao, Quantum kinetic theory of vibrational heating and bond breaking by hot electrons, *Phys. Rev. B: Condens. Matter Mater. Phys.*, 1997, **55**(3), 1876.
31 A. Tameshtit and J. E. Sipe, Positive quantum brownian evolution, *Phys. Rev. Lett.*, 1996, **77**(13), 2600.
32 L. Diósi, On high-temperature Markovian equation for quantum Brownian motion, *EPL*, 1993, **22**(1), 1.
33 A. Kossakowski, On quantum statistical mechanics of non-Hamiltonian systems, *Rep. Math. Phys.*, 1972, **3**, 247.
34 R. Durrett, *Probability: theory and examples*, Cambridge University Press, 2019, vol. 49.
35 L. Van Hove, Correlations in space and time and Born approximation scattering in systems of interacting particles, *Phys. Rev.*, 1954, **95**(1), 249.
36 J. Halliwell and A. Zoupas, Quantum state diffusion, density matrix diagonalization, and decoherent histories: A model, *Phys. Rev. D: Part. Fields*, 1995, **52**(12), 7294.
37 H. P. Breuer and F. Petruccione, *The theory of open quantum systems*, Oxford University Press on Demand, 2002.
38 D. J. Ward. *Spin-echo lineshapes in helium atom scattering from adsorbates*, PhD thesis, Cambridge University, 2013.
39 C. T. Chudley and R. J. Elliott, Neutron scattering from a liquid on a jump diffusion model, *Proc. Phys. Soc.*, 1961, **77**(2), 353.
40 S. W. Rick, D. L. Lynch and J. D. Doll, The quantum dynamics of hydrogen and deuterium on the Pd(111) surface: A path integral transition state theory study, *J. Chem. Phys.*, 1993, **99**, 8183.
41 T. Miyake, K. Kusakabe and S. Tsuneyuki, Inverse isotope effects in the surface diffusion of atoms, *Surf. Sci.*, 1996, **363**, 403–408.